Dalton Transactions

Accepted Manuscript

ROYAL SOCIETY OF CHEMISTRY

www.rsc.org/dalton

Dalton Transactions

Cite this: DOI: 10.1039/c0xx00000x

www.rsc.org/xxxxxx

PAPER

Switching of the photophysical properties of Bodipy-derived trans bis(tributylphosphine) Pt(II) bisacetylide complexes with rhodamine as the acid-activatable unit

Poulomi Majumdar, Xiaoneng Cui, Kejing Xu and Jianzhang Zhao*

Received (in XXX, XXX) Xth XXXXXXXXX 2014, Accepted Xth XXXXXXXXX 2014
DOI: 10.1039/b000000x

Rhodamine moiety was used for preparation of *trans* bis(tributylphosphine) Pt(II) bisacetylide complexes (**RH-BDPY-Pt-1** and **RH-BDPY-Pt-2**, with two different Bodipy acetylide ligands), which show acid/base-switchable photophysical properties. The rhodamine moiety undergoes reversible spirolactam↔opened amide structure transformation in the presence of acid/base. Bodipy ligands are responsible for strong visible light-harvesting. The photophysical properties of the Pt(II) complexes were studied with steady state UV–Vis absorption, luminescence spectra, nanosecond transient absorption spectroscopies, electrochemical characterization and DFT/TDDFT computations. In the absence of acid, the complexes show the absorption of Bodipy ligands at 580 nm and 500 nm, respectively. Both complexes show fluorescence. Minor phosphorescence band was observed for **RH-BDPY-Pt-1**. In the presence of trifluoroacetic acid (TFA), the spirolactam→opened amide transformation occurred and the absorption of rhodamine moiety at 570 nm appeared, colour changes were observed for the solution of the complexes. Moreover, the fluorescence of the complexes were switched on. Long-lived triplet excited states were observed for the two complexes (35 μs and 423 μs, respectively. In dichloromethane). Upon addition of TFA, the triplet state lifetime of **RH-BDPY-Pt-1** was substantially prolonged to 80 μs from 34 μs (the triplet state of **RH-BDPY-Pt-1** is localized on the Bodipy moiety); for **RH-BDPY-Pt-2**, however, the triplet state is switched from Bodipy-confined triplet state to a triplet state delocalized on the Bodipy and rhodamine moiety. Thus both the singlet excited state and the triplet state of the Pt(II) complexes were switched upon addition of acid. The photophysical properties were rationalized with DFT/TDDFT calculations. These results of tuning of the photophysical properties of Pt(II) complexes with rhodamine moiety may be useful for designing of external stimuli-activatable transition metal complexes.

Introduction

Triplet state photosensitizers are versatile compounds and have been widely used in photodynamic therapy (PDT) and oxygen sensing,[1–4] photocatalysis,[5–7] molecular logic gates,[8,9] etc. Recently switching of the triplet state become an emerging researching area because controllable population of the triplet state is of particularly interest for targeted PDT,[10–12] and molecular devices.[8] Controlling the vectorial energy transfer (EnT) process,[7] as well as the localization of the triplet state are fundamentally important for the mimic of photosynthesis, as well as for efficient photocatalysis.[7]

O'shea *et al.*[11] found that the singlet oxygen ($^1O_2$) photosensitizing ability of bromo-azaBodipy can be switched ON or OFF by changing the pH of solution. This method has been used for preparation of targeting PDT reagents which are able to be selectively activated by the acidic microenvironment of the tumour tissue.[13] Ziessel *at al*. studied the photoacid controlled vectorial fluorescence resonance energy transfer (FRET) with Bodipy-DPP triads (DPP = 1,4- oxo-3,6-diphenylpyrrolo[3,4-c]pyrrole), but the study is on singlet excited state manifold.[14] Akkaya *et al.* used acid-activated FRET to control the production of triplet excited state of Bodipy dyads, via the protonation of amino moiety attached on the Bodipy chromophore.[8] Photochromic moiety of diarylethene was also used to modulate the photophysical properties of Ir(III)[15], or Ru(II) and Pt(II) complexes,[16–19] etc. However, much room is still left to explore more mechanisms for switching of the photophysical properties of the triplet photosensitizers with diverse external stimuli.[20]

On the other hand, rhodamine is well known for its reversible transformation between the two tautomers, i. e. the spirolactam structure and the opened amide structure.[21,22] The two tautomers exhibit drastically different photophysical properties, with the former shows no visible light absorption

and no fluorescence. Conversely, strong absorption of visible light (ca. 555 nm) and fluorescence was observed for the opened amide form. The two tautomers are reversibly interchangeable with variation of the pH of solution. A wide variety of molecular sensors have been developed based on this reversible acid-activated tautomerism of rhodamine.[21–24] However, this reversible structure/photophysical property change was rarely used for switching of the triplet excited state. Previously, we prepared a rhodamine-containing Pt(II) complexes, but the structure of that specific rhodamine is unable to undergo the spirolactam/open form transformation.[25]

Herein, we prepared two rhodamine-containing Pt(II) complexes with different Bodipy ligands (**RH-BDP-Pt-1** and **RH-BDP-Pt-2**, Scheme 1). The two Bodipy ligands are with different coordination profile, thus different absorption wavelength was observed.[26] The Rhodamine moieties in the complexes are the acid-activatable units, thus we propose the photophysical properties of the complexes will be switched by addition of acid/base into the solutions. The photophysical properties of the complexes were studied with steady state UV–Vis absorption, luminescence spectra, nanosecond transient absorption spectroscopies, electrochemical characterization and DFT/TDDFT calculations. We found that the UV–Vis absorption, luminescence and triplet state properties of the complexes were reversibly switched by acid/base.

Experimental Section

Materials and reagents

All the chemicals are analytically pure and were used as received. ^{1}H and ^{13}C NMR spectra were recorded on a Bruker 400/500 MHz spectrophotometer ($CDCl_3$ as solvent, TMS as standard, δ = 0.00 ppm). High resolution mass spectra (HRMS) were determined with ESI-Q-TOF MS spectrometer. Fluorescence spectra were measured on a RF-5301PC spectrofluorometer (Shimadzu, Japan). Fluorescence quantum yields were measured with compound 5,10,15,20-tetraphenylporphyrin (TPP) as standard (Φ_F = 11% in toluene) and 2,6-diiodo-1,3,5,7-tetramethyl-8-phenyl-4,4-difluoroboradiazaindacene (diiodoBodipy, Φ_F = 2.7% in MeCN). Fluorescence lifetimes were measured with an OB920 spectrometer (Edinburgh, UK). Absorption spectra were recorded on an Agilent 8453A UV–Vis spectrophotometer.

Synthesis and characterization

Compound (**1**),[27] and Compound (**2**)[28] were synthesized according to the literature methods.

Compound rhodamine spirolactam (RH). Under Ar atmosphere, to a stirred solution of rhodamine B (402 mg, 0.84 mmol) in 1,2-dichloroethane (10 mL), prop-2-yn-1-amine (139 mg, 2.52 mmol) was added through syringe at 0 °C. To the mixture phosphorus oxychloride (0.3 mL, 3 mmol) was added dropwise. The mixture was stirred at 0 °C for 15 min, heated at 85 °C for 5 h, and then stirred at 25 °C for 24 hr. The solution was diluted with dichloromethane (20 mL) and acidified with 2 M HCl (30 mL). The organic layer was washed with 2 M HCl (2 × 30 mL), 2 M NaOH (3 × 30 mL), and brine (30 mL). The organic layer was dried over Na_2SO_4 and evaporated under reduced pressure. The product was purified by column chromatography (silica gel, Petroleum ether/EtOAc = 3:1, v/v) to give a light pink solid **RH.** Yield: 305 mg (75%). MP 188–190 °C. ^{1}H NMR (500 MHz, $CDCl_3$): δ 7.93–7.92 (m, 1H), 7.46–7.42 (m, 2H), 7.11–7.09 (m, 1H), 6.47 (d, 2H, *J* = 10 Hz), 6.39 (s, 2H), 6.27 (d, 2H, *J* = 10 Hz), 3.95 (s, 2H), 3.36–3.32(m, 8H), 1.75(s, 1H), 1.16 (t, 12H, *J* = 10 Hz). ^{13}C NMR (125 MHz, $CDCl_3$): δ 167.51, 153.91, 153.63, 149.02, 132.76, 130.59, 129.25, 128.13, 123.93, 123.15, 108.16, 105.28, 97.97, 78.45, 70.16, 64.93, 44.53, 28.67, 12.73. TOF HRMS ES$^+$: calcd ($[C_{31}H_{33}N_3O_7 + H]^+$), *m/z* = 480.2651, found, *m/z* = 480.2645.

Compound BDPY-Pt-1. Under Ar atmosphere, a round bottom flask containing a stirred solution of compound **1** (34.8 mg, 0.1 mmol) and *cis*-Pt[P(*n*-Bu)$_3$]$_2$Cl$_2$ (80 mg, 0.12 mmol) in THF/Et_2NH (1:1, v/v, 6 mL), was placed in a Dewar flask (ethyl acetate/liquid nitrogen low temperature bath). The flask was evacuated and back-filled with Ar for several times. Then CuI (3.8 mg, 0.02 mmol) was added to the mixture. The temperature of the mixture was allowed to rise from –78 °C to RT and stirred at RT. The reaction was monitored by TLC (CH_2Cl_2/Petroleum ether = 1:2 as eluent, v/v). After consumption of almost all of the starting materials, deionized water was used to quench the reaction. The mixture was extracted with dichloromethane (3× 25 mL). Organic phase was dried over Na_2SO_4, the solvent was evaporated under reduced pressure, and the crude products thus obtained was purified by column chromatography (silica gel, CH_2Cl_2/petroleum ether = 1:2, v/v) to give **BDPY-Pt-1** as a purple solid. Yield: 75 mg (77 %). MP 90–92 °C. ^{1}H NMR (400 MHz, $CDCl_3$): 7.48–7.28 (m, 5H), 5.93 (s, 1H), 2.64 (s, 3H), 2.53 (s, 1H), 1.93 (s, 12H), 1.43–1.35 (m, 30H), 0.89 (t, 18H, *J* =8.0 Hz). ^{13}C NMR (100 MHz, $CDCl_3$): δ 158.4, 154.1, 142.0, 140.9, 140.7, 135.5, 131.5, 131.1, 129.2, 129.0, 128.2, 122.2, 120.7, 92.0, 90.0, 29.9, 26.3, 24.4, 22.2, 22.1, 21.9, 14.4, 14.0, 13.3. MALDI-HRMS: calcd ($[C_{45}H_{72}BClF_2N_2P_2Pt]^+$), *m/z* = 981.4568, found, *m/z* = 981.4590.

Compound BDPY-Pt-2. Under Ar atmosphere, a stirred solution of compound **2** (34.8 mg, 0.1 mmol) and *cis*-Pt[P(n-Bu)$_3$]$_2$Cl$_2$ (79.6 mg, 0.12 mmol) in Et_2NH (8 mL) was refluxed at 45 °C for 8 h. Then the reaction mixture was cooled to RT and the solvent was removed under reduced pressure. The crude product thus obtained, was purified by column chromatography (silica gel, CH_2Cl_2/petroleum ether = 1 : 1, v/v) to give a orange solid. Yield: 58 mg (59 %). MP 119–121°C. ^{1}H NMR (400 MHz, $CDCl_3$): 7.35–7.08 (m, 4H), 5.97 (s, 2H), 2.55 (s, 6H), 2.04 (s, 12H), 1.59 (m, 12H), 1.49–1.40 (m, 18H), 0.92 (t, 18H, *J* = 8.0 Hz). ^{13}C NMR (100 MHz, $CDCl_3$): δ 155.4, 143.3, 142.3, 131.6, 129.8, 127.7, 121.2, 106.2, 86.2, 86.0, 85.9, 29.9, 26.3, 24.6, 24.5, 24.4, 22.4, 22.3, 22.1, 14.7, 13.9. MALDI-HRMS: calcd ($[C_{45}H_{72}BClF_2N_2P_2Pt]^+$), *m/z* =981.4568, found, *m/z* =981.4577.

Compound RH-Pt. Under Ar atmosphere, to a stirred solution of **RH** (28.8 mg, 0.06 mmol) and *cis*-Pt[P(n-Bu)$_3$]$_2$Cl$_2$ (40.2 mg, 0.06 mmol) in CH_2Cl_2 (10 mL), diisopropylamine (2 mL) and CuI (3.0 mg, 0.015 mmol) were added consecutively. The mixture was stirred at 25 °C for 18 h. Then the solvent was removed under reduced pressure. The crude product thus obtained was purified by column chromatography (silica gel, petroleum ether/EtOAc = 4:1, v/v) to give a colourless oil. Yield: 20 mg (30 %). ^{1}H NMR (500 MHz, $CDCl_3$): 7.85–7.84 (m, 1H), 7.34 (m, 2H), 6.98–6.96 (m, 1H), 6.61 (d, 2H, *J* = 10 Hz), 6.38 (s, 2H),

6.25 (d, 2H, *J* = 10 Hz), 3.96 (s, 2H), 3.36–3.28 (m, 8H), 1.88–1.85 (m, 12H), 1.46–1.43 (m, 12H), 1.40–1.33 (m, 12H), 1.16 (t, 12H, *J* = 10 Hz), 0.87 (t, 18H, *J* = 10 Hz). ^{13}C NMR (125 MHz, $CDCl_3$): *δ* 168.14, 154.84, 153.34, 148.68, 132.17, 130.32, 128.91, 127.68, 123.45, 122.84, 107.88, 106.17, 98.09, 93.78, 65.23, 44.46, 32.65, 29.87, 26.39, 26.16, 24.45, 24.38, 24.31, 23.95, 23.78, 22.08, 21.92, 21.75, 14.00, 12.87. MALDI-HRMS: calcd ($[C_{55}H_{86}ClN_3O_2P_2Pt + H]^+$), *m/z* = 1113.5610, found, *m/z* =1113.5522.

Compound RH-BDPY-Pt-1. Under Ar atmosphere, to a stirred solution of **RH** (24.0 mg, 0.05 mmol) and **BDPY-Pt-1** (49.1 mg, 0.05 mmol) in CH_2Cl_2 (10 mL), diisopropylamine (2 mL) and CuI (3.8 mg, 0.02 mmol) were added consecutively. The mixture was stirred at 25 °C for 24 h. Then the solvent was removed under reduced pressure. The crude product thus obtained, was purified by column chromatography (silica gel, petroleum ether/EtOAc = 4:1, v/v) to give a purple solid. Yield: 35 mg (49 %). MP 82–84 °C. ^{1}H NMR (500 MHz, $CDCl_3$): 7.93–7.87 (m, 1H), 7.47–7.46 (m, 3H), 7.41–7.34 (m, 2H), 7.25–7.24 (m, 2H), 6.99–6.98 (m, 1H), 6.61–6.55 (m, 2H), 6.37 (s, 2H), 6.28–6.26 (m, 2H), 5.92 (s, 1H), 3.94 (s, 2H), 3.39–3.27 (m, 8H), 2.61 (s, 3H), 2.52 (s, 3H), 1.94–1.91 (m, 12H), 1.45–1.43 (m, 12H), 1.34–1.30 (m, 15H), 1.16 (t, 12H, *J* = 10 Hz), 0.87–0.82 (m, 21H). ^{13}C NMR (125 MHz, $CDCl_3$): *δ* 167.95, 159.34, 154.75, 153.18, 152.84, 148.50, 140.94, 140.75, 140.13, 135.47, 131.91, 131.04, 130.91, 130.26, 128.92, 128.71, 128.16, 127.44, 123.25, 122.90, 122.70, 120.08, 117.44, 107.74, 106.23, 101.53, 98.96, 97.98, 94.69, 65.10, 44.29, 32.43, 31.94, 29.71, 29.37, 29.68, 24.29, 24.23, 24.18, 23.73, 23.60, 23.46, 22.70, 14.40, 14.20, 13.84, 13.28, 12.71. MALDI-HRMS: calcd ($[C_{76}H_{104}BF_2ClN_5O_2P_2Pt + H]^+$), *m/z* =1425.7452, found, *m/z* =1425.7397.

Compound RH-BDPY-Pt-2. Under Ar atmosphere, to a stirred solution of **RH** (24.0 mg, 0.05 mmol) and **BDPY-Pt-2** (49.1 mg, 0.05 mmol) in CH_2Cl_2 (10 mL) at 25 °C, diisopropylamine (2 mL) and CuI (3.8 mg, 0.02 mmol) were added consecutively. The reaction was monitored by TLC (silica gel, petroleum ether/EtOAc = 4:1 , v/v). After consumption of all the starting materials, the solvent was removed under reduced pressure. The crude product thus obtained was purified by column chromatography (silica gel, petroleum ether/EtOAc = 4:1, v/v) to give a sticky orange solid. Yield: 34 mg (48 %). ^{1}H NMR (500 MHz, $CDCl_3$): 7.86–7.82 (m, 1H), 7.35–7.32 (m, 4H), 7.05 (d, 2H, *J* = 10 Hz), 6.99–6.97 (m, 1H), 6.64 (d, 2H, *J* = 10 Hz), 6.38 (m, 2H), 6.25 (d, 2H, *J* = 10 Hz), 5.95 (s, 2H), 3.97(s, 2H), 3.38–3.29 (m, 8H), 2.54 (s, 6H), 2.03–2.00 (m, 12H), 1.52–1.48 (m, 12H), 1.43(s, 6H), 1.40–1.33 (m, 12H), 1.17 (t, 12H, *J* = 10 Hz), 0.86 (t, 18H, *J* = 10 Hz). ^{13}C NMR (125 MHz, $CDCl_3$): *δ* 168.03, 155.11, 154.77, 153.21, 148.55, 143.28, 142.49, 131.94, 131.50, 131.43, 130.77, 130.20, 130.11, 128.75, 127.47, 127.39, 123.25, 122.68, 120.99, 112.13, 108.26, 107.74, 106.25, 101.60, 98.01, 94.68, 65.17, 44.29, 32.47, 31.93, 29.70, 29.36, 26.31, 24.38, 24.32, 24.25, 23.97, 23.81, 23.64, 22.69, 14.56, 14.12, 13.80, 12.73. MALDI-HRMS: calcd ($[C_{76}H_{104}BF_2ClN_5O_2P_2Pt + H]^+$), *m/z* =1425.7452, found, *m/z* =1425.7539.

Nanosecond transient absorption spectra

All the nanosecond transient absorption spectra were measured on LP920 laser flash photolysis spectrometer (Edinburgh Instruments, UK) and recorded on a Tektronix TDS 3012B oscilloscope. The lifetime values (by monitoring the decay trace of the transients) were obtained with the LP900 software. All samples in flash photolysis experiments were deaerated with N_2 for ca. 15 min before measurement and the gas flow is kept during the measurement. For the samples with TFA added, the solution was allowed to stand for 8 min prior to measurement.

Cyclic voltammetry

Cyclic voltammetry was performed using a CHI610D Electrochemical workstation (Shanghai, China). Cyclic voltammograms were recorded at scan rates of 0.1 V/s. The electrolytic cell used was a three electrodes cell. Electrochemical measurements were performed at RT using 0.1 M tetrabutylammonium hexafluorophosphate ($Bu_4N[PF_6]$) as supporting electrolyte. The solution was purged with N_2 before measurement. The working electrode was a glassy carbon electrode, and the counter electrode was platinum electrode. A non aqueous $Ag/AgNO_3$ (0.1 M in acetonitrile) reference electrode was contained in a separate compartment connected to the solution via semipermeable membrane. Dichloromethane was used as the solvent. Ferrocene was added as the internal references.

DFT calculations

The density functional theory (DFT) calculations were used for optimization of both singlet states and triplet states. The UV–Vis absorption and the energy level of the T_1 state were calculated with the time dependent DFT (TDDFT), based on the optimized singlet ground state geometries (S_0 state). The spin density surface of the complexes were calculated based on the optimized triplet state. All the calculations were performed at the B3LYP/GENECP/LANL2DZ level with Gaussian 09W.[29] Dichloromethane was used as the solvent for the calculations (CPCM model).

Results and Discussions

Design and Synthesis of the Pt(II) complexes

2-EthynylBodipy and meso-4'-ethylBodipy were used for preparation of the complexes, in order to attain strong absorption of visible light.[30–32] Furthermore, the absorption wavelength of the two coordinated ligands are different, thus singlet EnT process in the two complexes may be different.[33] The rhodamine moiety was connected to the Pt(II) coordination centre via acetylide ligands. In order to feasibly attach two different acetylide ligands to Pt(II) coordination centre, the *trans* bis(tributylphosphine) Pt(II) bisacetylides coordination framework was selected.[34–38] Complexes **RH-Pt**, **BDPY-Pt-1** and **BDPY-Pt-2** were prepared as reference complexes (Scheme 1). The preparation of the ligands and the complexes are based on routine methods. The compounds were obtained with moderate yields.

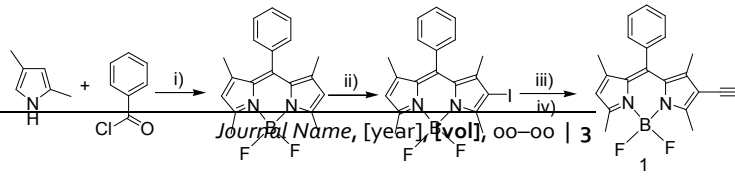

1

Scheme 1. Synthetic of the rhodamine-Bodipy-Pt(II) complexes. Compound **B-6** and 4-dicyanomethylene-2-methyl-6-p-dimethylaminostyryl-4H-pyran (DCM) used as the standard for the fluorescence quantum yields are also presented. Reagents and conditions: (i) Dry CH_2Cl_2, $BF_3{\cdot}OEt_2$, NEt_3; (ii) NIS, RT; (iii) trimethylsilylacetylene, $Pd(PPh_3)_2Cl_2$, PPh_3, CuI, NEt_3, reflux, 8 h; (iv) K_2CO_3, THF:MeOH (1:1, v/v), RT, 20 min; (v) K_2CO_3, MeOH, RT, 3 h; (vi) dry CH_2Cl_2, CF_3COOH, $BF_3{\cdot}OEt_2$, NEt_3; (vii) Under Ar, 1,2-dichloroethane, $POCl_3$, 85 °C, reflux, 4 h. (viii) Under Ar, 1,2-dichloroethane, rhodamine B acid chloride, RT, 24 h. (ix) distilled THF, $NHEt_2$, CuI, –78 °C to RT, stirred; (x) $NHEt_2$, 45 °C , 8 h; (xi) dry CH_2Cl_2, CuI, *i*-Pr_2NH, 25°C.

UV–Vis absorption spectra and the Luminescence spectra

RH-Pt shows absorption band at 311 nm (Fig. 1). No absorption in visible spectra region was observed. For **BDPY-Pt-1** and **BDPY-Pt-2**, strong absorption at 570 nm and 500 nm were observed, respectively. The UV–Vis absorption of **RH-BDPY-Pt-1** shows an absorption spectra which is superimposition to the sum of the absorption spectra of two components. Thus, we propose there is no significant interaction between the rhodamine (in the spirolactam structure) and the Bodipy moiety. Similar results were observed for **RH-BDPY-Pt-2** (Fig. 1). Notably the different coordination profile of the Bodipy ligands in **RH-BDPY-Pt-1** and **RH-BDPY-Pt-2** give drastically different absorption wavelength.[26]

The UV–Vis absorption of complexes does not show significant solvent dependency, indicating that the ground state were not affected by the solvent polarity or hydrogen bonding (see ESI †, Fig. S21).

The UV–Vis absorption of the complexes changed on addition of acid (TFA), thus the spirolactam↔opened amide form transformation was occurred (Fig. 2). For **RH-BDPY-Pt-1**, the absorption maxima was blue-shifted to 558 nm upon addition of TFA (Fig. 2a). For **RH-BDPY-Pt-2**, however, a new absorption band at longer wavelength (555 nm) (Fig. 2b) was observed upon addition of TFA, which is attributed to the absorption of the opened amide form of the rhodamine moiety. This postulation was supported by the change of UV–Vis absorption of the reference complex **RH-Pt** (Fig. 2c).

The colour of the complexes solution changed upon addition of TFA (Fig. 2d-2f). For example, **RH-BDPY-Pt-1** gives purple colour solution whereas upon addition of TFA, magenta solution was obtained. **RH-BDPY-Pt-2** also shows different colour changes. **RH-BDPY-Pt-2** alone in solution shows dark yellow

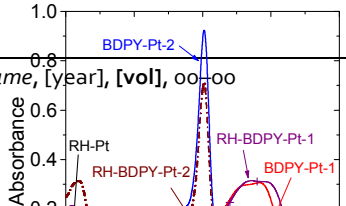

Fig. 1 UV–Vis absorption spectra of **BDPY-Pt-1**, **RH-BDPY-Pt-1**, **BDPY-Pt-2**, **RH-BDPY-Pt-2** and **RH-Pt**. $c = 1.0 \times 10^{-5}$ M in toluene. 20 °C.

colour, upon addition of TFA, pinkish orange solution was obtained. These changes are different from **RH-Pt**, which shows a colourless light pink change upon addition of TFA. To the best of our knowledge, such tuning of the colour of Pt(II) complexes is rarely reported, and application of rhodamine chromophore in tuning the colour of Pt(II) complexes was never reported.[22,39]

The photoluminescence spectra of the complexes were studied. Complex **BDPY-Pt-1** gives a major emission band at 629 nm (Fig 3a). The emission intensity is the same in both aerated and deaerated solution. Thus the luminescence is fluorescence. A minor emission band was observed at 800 nm for **BDPY-Pt-1.** The intensity of this minor band was reduced in aerated solution, indicating the emission band is most likely originated from a emissive triplet state, thus the emission at 800 nm is phosphorescence.[26] Similar results were observed for **RH-BDPY-Pt-1** (Fig 3b). For **BDPY-Pt-2**, however, the emission profile is drastically different. An emission band at 517 nm was observed (Fig 3c). No phosphorescence emission band was observed. Similar results were found for **RH-BDPY-Pt-2** (Fig 3d). These results indicate that the coordination profile of the acetylide ligands impose substantial effect on the photophysical properties of the complexes. Furthermore, the rhodamine moiety in the spirolactam structure does not contribute to the photoluminescence of the complexes.

Fig. 3 Emission spectra of the complexes (a) **BDPY-Pt-1** (λ_{ex} = 555 nm), (b) **RH-BDPY-Pt-1** (λ_{ex} = 555 nm), (c) **BDPY-Pt-2** (λ_{ex} = 470 nm), and (d) **RH-BDPY-Pt-2** (λ_{ex} = 470 nm) at different atmosphere of air, N_2, and O_2. $c = 1.0 \times 10^{-5}$ M in toluene. 20 °C.

The solvent-dependency of the emission spectra of the complexes was studied (Fig. 4). The fluorescence emission intensity of **BDPY-Pt-1** (Fig. 4a) decreased in polar solvents as compared with that in nonpolar solvents. Similar profile was found for **RH-BDPY-Pt-1** (Fig. 4b). The emission intensity of **BDPY-Pt-2** also decreased in polar solvents (Fig. 4c). More significant solvent polarity-dependent photoluminescence was observed for **RH-BDPY-Pt-2** (Fig. 4d). These polarity dependent emission indicates intramolecular charge transfer feature of the emissive state.

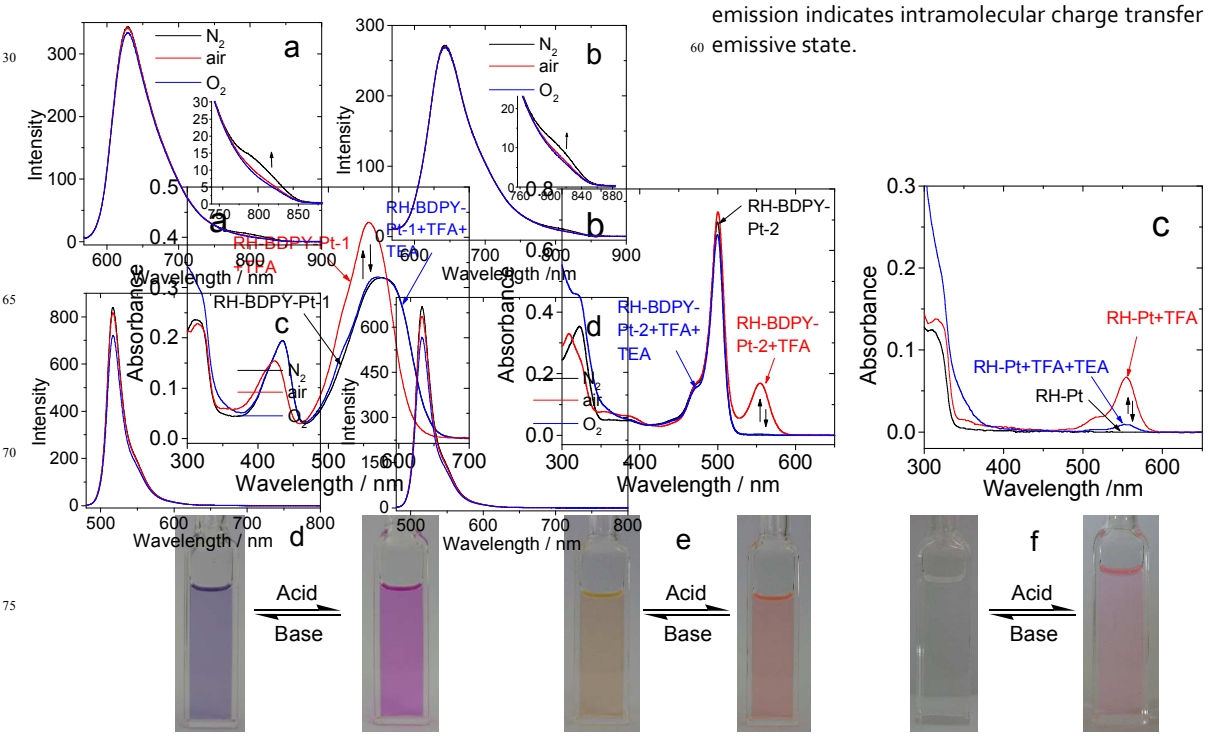

Fig. 2 UV–Vis absorption spectra of complexes in the absence and in the presence of TFA. (a) **RH-BDPY-Pt-1**, **RH-BDPY-Pt-1**+TFA (333 eqv.) and **RH-BDPY-Pt-1**+TFA (333.3 eqv.) + TEA (pure 150 μL). (b) **RH-BDPY-Pt-2**, **RH-BDPY-Pt-2**+TFA (333 eqv.) and **RH-BDPY-Pt-2**+TFA (333 eqv.) + **TEA** (neat, 500 μL). (c) **RH-Pt**, **RH-Pt**+TFA (333 eqv. and 8 min standing time), **RH-Pt-1**+TFA (333 eqv.)+**TEA** (neat, 250 μL). Color changes of the complexes on addition of acid (TFA, 333 eqv.) and base (TEA): (d) **RH-BDPY-Pt-1**, (e) **RH-BDPY-Pt-2**, and (f) **RH-Pt**. $c = 1.0 \times 10^{-5}$ M in dichloromethane. 20 °C.

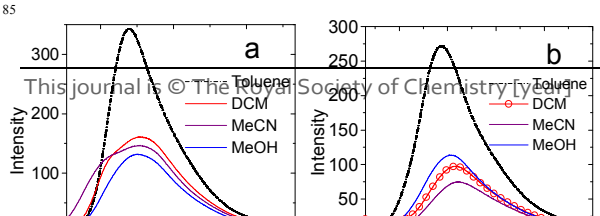

Fig. 4 Solvent-polarity-dependence of the emission of the complexes (c = 1.0 × 10^{-5} M): (a) **BDPY-Pt-1** (λ_{ex} = 555 nm), (b) **RH-BDPY-Pt-1** (λ_{ex} = 555 nm), (c) **BDPY-Pt-2** (λ_{ex} = 470 nm), and (d) **RH-BDPY-Pt-2** (λ_{ex} = 470 nm). 20 °C.

The photoluminescence spectra of the complexes upon addition of acid were studied (Fig. 5). For **RH-BDPY-Pt-1**, a new emission band at 598 nm developed upon addition of TFA. Notably the emission wavelength is shorter than the fluorescence emission of the Pt(II) coordination centre of **RH-BDPY-Pt-1**. The emission intensity of **RH-BDPY-Pt-1** in the presence of TFA was found to be weaker as compared to **RH-Pt** in the presence of TFA, most probably due to FRET (see ESI†, Fig. S22). For **RH-BDPY-Pt-2**, the emission of the coordinated Bodipy at 500 nm was greatly enhanced upon photoexcitation. Thus we propose that the non-radiative decay channel of **RH-BDPY-Pt-2** in DCM, such as intramolecular charge transfer, was inhibited upon addition of TFA.

Furthermore, a new emission band at 573 nm was observed, which is attributed to the opened amide structure of the rhodamine moiety. This conclusion was supported by the results with **RH-Pt** (Fig. 5c). Switch-ON effect was observed for complexes upon the spirolactam↔opened amide transformation. These complexes may be developed for dual functional materials for selective luminescence bioimaging and PDT study.[21]

In order to study the FRET in the complexes upon addition of TFA, the fluorescence excitation spectra of the complexes were compared with the UV–Vis absorption spectra of the complexes (Fig. 6). For **RH-BDPY-Pt-2**, an excitation band at 502 nm was observed, indicating the presence of FRET. We noted the much weak excitation band at 502 nm as compared to the UV–Vis absorption band of the complex at the same region. This discrepancy may be partially due to the inefficient spirolactam↔ opened amide structure transformation.

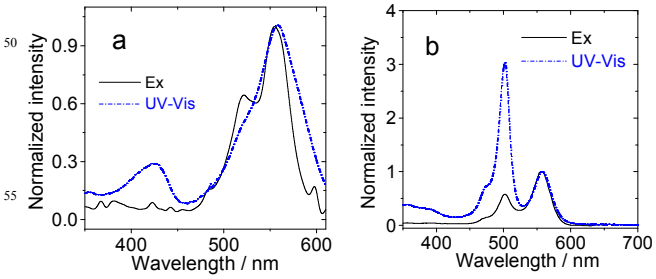

Fig. 6 Comparison of the normalized UV–vis absorption and the excitation spectra of the complexes. (a) **RH-BDPY-Pt-1** (λ_{em} = 600 nm), c[**RH-BDPY-Pt-1**] = 5.0 ×10^{-6} M and (b) **RH-BDPY-Pt-2** (λ_{em} = 580 nm), c[**RH-BDPY-Pt-2**] = 3.3 ×10^{-6} M. In presence of TFA (333 eqv.). The concentration was adjusted so that the absorbance at the maximal absorption band is less than 0.2. In deaerated dichloromethane. 20 °C .

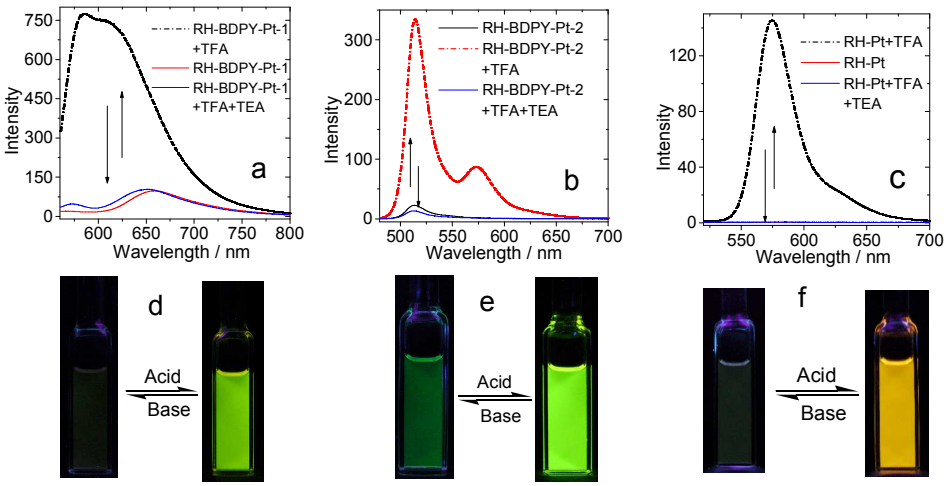

Fig. 5 Emission spectra of (a) **RH-BDPY-Pt-1**, **RH-BDPY-Pt-1**+TFA (333 eqv.) and **RH-BDPY-Pt-1**+TFA (333 eqv. and 8 min standing time)+TEA (pure 150 μL) (λ_{ex} = 550 nm). (b) **RH-BDPY-Pt-2**, **RH-BDPY-Pt-2**+TFA (333 eqv.) and **RH-BDPY-Pt-2**+TFA (333 eqv.)+**TEA** (pure 500 μL) (λ_{ex} = 470 nm). (c) **RH-Pt**, **RH-Pt**+TFA (333 eqv. and 8 min standing time), **RH-Pt-1**+TFA (333 eqv.)+TEA (pure 250 μl) (λ_{ex} = 510 nm). c = 1.0 ×10^{-5} M. 20 °C in dichloromethane. Colour changes of the complexes under UV hand lamp (λ_{ex} = 365 nm) on addition of acid (TFA, 333 eqv.) and base (TEA): (d) **RH-BDPY-Pt-1**, (e) **RH-BDPY-Pt-2**, and (f) **RH-Pt**. c = 1.0 ×10^{-5} M in dichloromethane. 20 °C.

Table 1. Photophysical properties of Pt(II) Complexes [a]

		λ_{abs} / nm	ε [b]	λ_{em} / nm	τ_F [c] / ns	Φ_F [d] / %	τ_T [g] / μs	Φ_Δ / %
RH-Pt	Toluene	311	1.19	[j]	[j]	[j]	[j]	[j]
	DCM	311	1.22	[j]	[j]	[j]	[j]	[j]
	Acetonitrile	311	1.17	[j]	[j]	[j]	[j]	[j]
	Methanol	311	1.22	[j]	[j]	[j]	[j]	[j]
BDPY-Pt-1	Toluene	432/583	1.38/3.0	629	0.3	1.6 [e]	57	15 [h]
	DCM	428/570	1.58/3.10	641	0.2	0.9 [e]	46	48 [h]
	Acetonitrile	427/562	1.70/3.3	641	0.2	0.6 [e]	37	22 [h]
	Methanol	425/562	1.63/3.521	638	0.2	0.5 [e]	20	7.8 [h]
BDPY-Pt-2	Toluene	503	9.26	517	2.6	25.4 [f]	598	21 [i]
	DCM	500	8.78	514	0.8	4.4 [f]	363	60 [i]
	Acetonitrile	496	8.58	509	1.4	0.9 [f]	254	66 [i]
	Methanol	497	8.73	510	1.1	3.2 [f]	440	34 [i]
RH-BDPY-Pt-1	Toluene	319/438/594	2.02/1.73/3.10	643	0.3	0.6 [e]	52	18 [h]
	DCM	315/436/580	2.46/2.05/3.36	653	0.2	0.9 [e]	35	35 [h]
	Acetonitrile	318/433/573	2.36/1.97/3.28	659	0.2	0.3 [e]	31	21 [h]
	Methanol	314/433/566	2.30/1.88/3.47	653	0.3	0.4 [e]	12	6.7 [h]
RH-BDPY-Pt-2	Toluene	320/502	3.12/7.13	516	2.4	16.3 [f]	618	9.2 [i]
	DCM	323/500	3.34/6.54	512	1.0	0.6 [f]	423	72 [i]
	Acetonitrile	318/497	3.43/7.21	510	1.4	0.6 [f]	328	59 [i]
	Methanol	322/496	3.59/6.79	509	0.5	0.9 [f]	331	22 [i]
RH-Pt+TFA	DCM	320/555	1.35/0.67	575	3.5	54.8 [e]	[j]	[j]
RH-BDPY-Pt-1+TFA	DCM	317/423/558	2.27/1.53/4.29	598	3.0	3.8 [e]	80	34 [i]
RH-BDPY-Pt-2+TFA	DCM	309/500/555	3.31/7.25/1.70	513/573	1.79	32.2 [e] /9.4 [f]	406	16 [h] /51 [i]

[a] c = 1.0 × 10^{-5} M. [b] Molar extinction coefficient at the absorption maxima. ε: 10^5 M^{-1} cm^{-1}. [c] Fluorescence lifetimes in aerated solution. [d] Fluorescence quantum yields. [e] Fluorescence quantum yields with **B-6** (Φ_F = 10.5 % in toluene) and [f] **DCM** (Φ_F = 10% in CH_2Cl_2) as the standard. [g] Triplet excited state lifetimes, measured by nanosecond transient absorption spectra under N_2 atmosphere (c = 1.0 × 10^{-5} M in toluene). Singlet oxygen quantum yields: [h] with Methylene blue (**MB**. Φ_Δ = 57% in DCM) and [i] 2,6-diiodo-Bodipy (Φ_Δ = 83% in DCM) as standard. The excitation wavelength, for **BDPY-Pt-1** (λ_{ex} = 592 nm), **RH-BDPY-Pt-1** (λ_{ex} = 592 nm), **BDPY-Pt-2** (λ_{ex} = 514 nm), **RH-BDPY-Pt-2** (λ_{ex} = 514 nm) in toluene; for **BDPY-Pt-1** (λ_{ex} = 592 nm), **RH-BDPY-Pt-1** (λ_{ex} = 592 nm), **BDPY-Pt-2** (λ_{ex} = 488 nm), **RH-BDPY-Pt-2** (λ_{ex} = 488 nm) in CH_2Cl_2; for **BDPY-Pt-1** (λ_{ex} = 588 nm), **RH-BDPY-Pt-1** (λ_{ex} = 588 nm), **BDPY-Pt-2** (λ_{ex} = 506 nm), **RH-BDPY-Pt-2** (λ_{ex} = 506 nm) in acetonitrile and methanol; [j] Not determined.

Nanosecond transient absorption spectra

The nanosecond transient absorption spectra of the complexes were studied (Fig. 7).[4,40,41] **BDPY-Pt-1** gives a significant bleaching band at 560 nm, and excited state absorption (ESA) in the region of 300 – 500 nm (Fig. 7a). Thus the triplet state of **BDPY-Pt-1** is localized on the Bodipy ligand (^{3}IL state).[26,40c,42] The lifetime was determined as 56 μs (Fig. 7b). For **BDPY-Pt-2**, however, the bleaching band is at 500 nm (Fig. 7c), and the lifetime of the triplet state is up to 598 μs (Fig. 7d). The TA spectra of the rhodamine-containing complexes **RH-BDPY-Pt-1** and **RH-BDPY-Pt-2** were also studied. **RH-BDPY-Pt-1** shows similar transient spectrum (Fig. 7e) with that of **BDPY-Pt-1**. The triplet state lifetime 52 μs (Fig. 7f) is also close to that of **BDPY-Pt-1**. Therefore, the rhodamine moiety in the spirolactam structure in **RH-BDPY-Pt-1** does not impose any effect on the triplet state of **RH-BDPY-Pt-1**. Moreover, based on the bleaching band, we conclude that the triplet state of **RH-BDPY-Pt-1** is localized on the Bodipy moiety, not on the spirolactam rhodamine moiety.[43] For **RH-BDPY-Pt-2**, the transient absorption spectra is similar to that of **BDPY-Pt-2**, the triplet state lifetime of **RH-BDPY-Pt-2** is up to 618 μs.[40c]

The variation of the TA spectra upon addition of acid (TFA) was also studied (Fig. 8). Dichloromethane (DCM) was used as the solvent since the spirolactam↔opened amide structure transformation is retarded in toluene. The lifetime of the triplet excited state of **BDPY-Pt-1** in DCM (46 μs) is slightly shorter than that in toluene (57 μs). In the presence of TFA, no significant change of the TA spectra and the lifetime of the triplet excited state (45 μs) (see ESI †, Fig. S23).

For **RH-BDPY-Pt-1**, the triplet state lifetime in DCM is 34 μs. Upon addition of TFA, no substantial changes were observed for the TA spectra. However, the triplet state lifetime was significantly extended to 80 μs. Thus switching of the triplet state lifetime was observed for **RH-BDPY-Pt-1** upon addition of TFA. Interestingly, the triplet state of **RH-BDPY-Pt-1** is still localized on the Bodipy moiety, not the rhodamine moiety. This localization profile was attributed to the higher triplet state energy level of rhodamine than that of Bodipy moiety.[41a]

BDPY-Pt-2 shows much shorter triplet state lifetime in DCM than that in toluene (Fig. 9). Similar results were observed for **RH-BDPY-Pt-2**. This reduced triplet state lifetime in polar solvent may be due to intramolecular charge transfer.[44] Notably the triplet state is still localized on the Bodipy moiety. Upon addition of TFA, a new bleaching band at 553 nm was observed in the TA spectra of **RH-BDPY-Pt-2** (Fig. 9e). This band can be attributed to the population of the rhodamine-localized triplet state. A major bleaching band at 500 nm was observed, which can be attributed to the ground state bleaching of the Bodipy ligand. The decay kinetics of the two bleaching bands were studied. Different lifetime of 406 μs and 35 μs were observed. This result indicate that there is no efficient triplet state equilibrium in **RH-BDPY-Pt-2**.[41,45] The TA spectra of **RH-Pt** in the presence of TFA was also studied. A very long-lived triplet

excited state with lifetime up to 985 μs was observed. Based on the triplet state lifetimes, the intramolecular triplet state EnT rate constant in **RH-BDPY-Pt-2**[34,40a] can be calculated as 2.8 × 10^4 s^{-1} with Eq. 1:

$$k_{ET} = \left(\frac{1}{\tau}\right) - \left(\frac{1}{\tau_e^\circ}\right) \quad \text{(Eq. 1)}$$

where, τ_e and τ°_e are the emission lifetimes of the donor in the presence and absence of an energy acceptor, respectively.

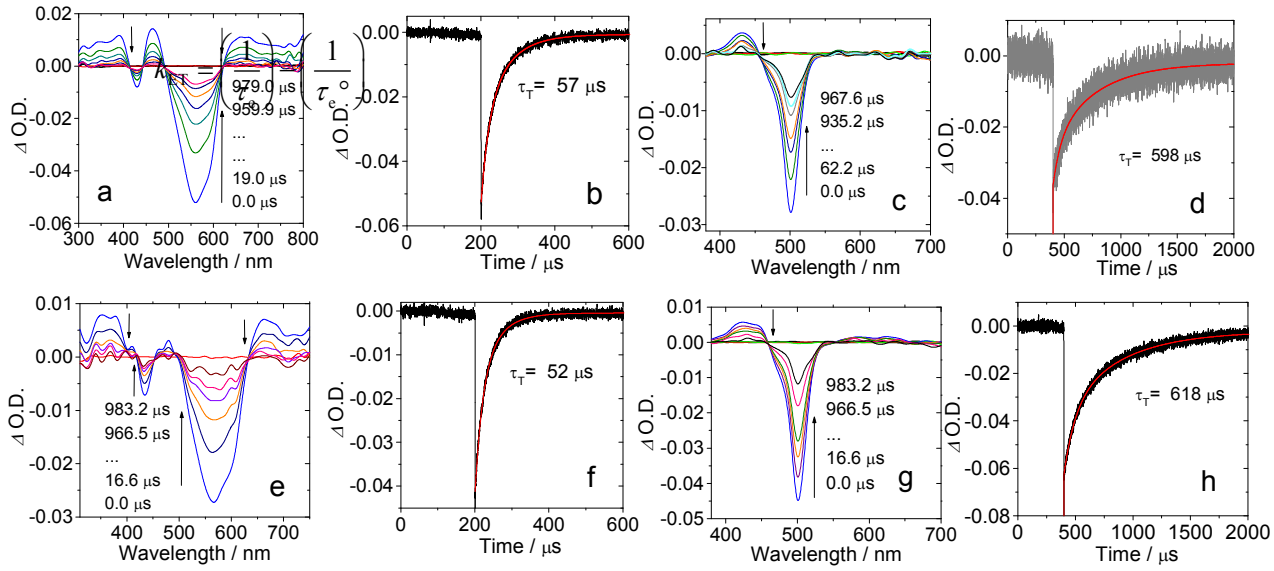

Fig. 7 Nanosecond transient absorption spectra and the decay curves of the complexes. (a) **BDPY-Pt-1** and (b) decay curve of **BDPY-Pt-1** at 584 nm (λ_{ex} = 532 nm), (c) **BDPY-Pt-2** and (d) decay curve of **BDPY-Pt-2** at 504 nm (λ_{ex} = 500 nm), (e) **RH-BDPY-Pt-1**, (f) decay curve of **RH-BDPY-Pt-1** at 584 nm (λ_{ex} = 532 nm), (g) **RH-BDPY-Pt-2** and (h) decay curve of **RH-BDPY-Pt-2** at 504 nm (λ_{ex} = 500 nm). c = 1.0 × 10^{-5} M in deaerated toluene, 20 °C.

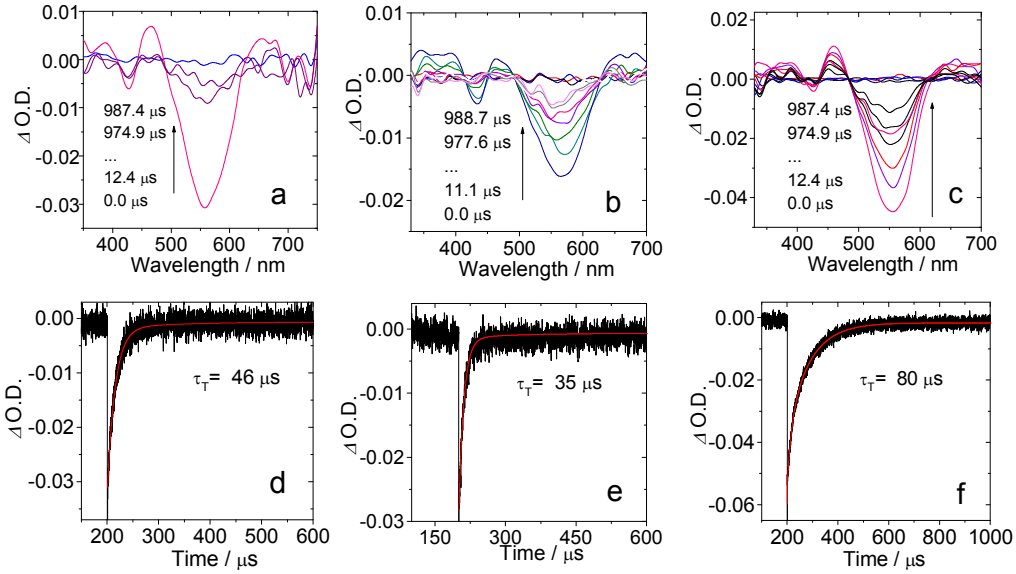

Fig. 8 Nanosecond transient absorption spectra and the decay curves of complexes. Transient absorption spectra of (a) **BDPY-Pt-1**, (b) **RH-BDPY-Pt-1** and (c) **RH-BDPY-Pt-1**+TFA (333 eqv.), the corresponding decay curves of (d) **BDPY-Pt-1** at 580 nm (λ_{ex} = 532 nm), (e) **RH-BDPY-Pt-1** at 584 nm (λ_{ex} = 532 nm) and (f) decay curve of **RH-BDPY-Pt-1**+TFA (333 eqv.) at 557 nm (λ_{ex} = 532 nm). c = 1.0 ×10^{-5} M in deaerated dichloromethane, 20 °C.

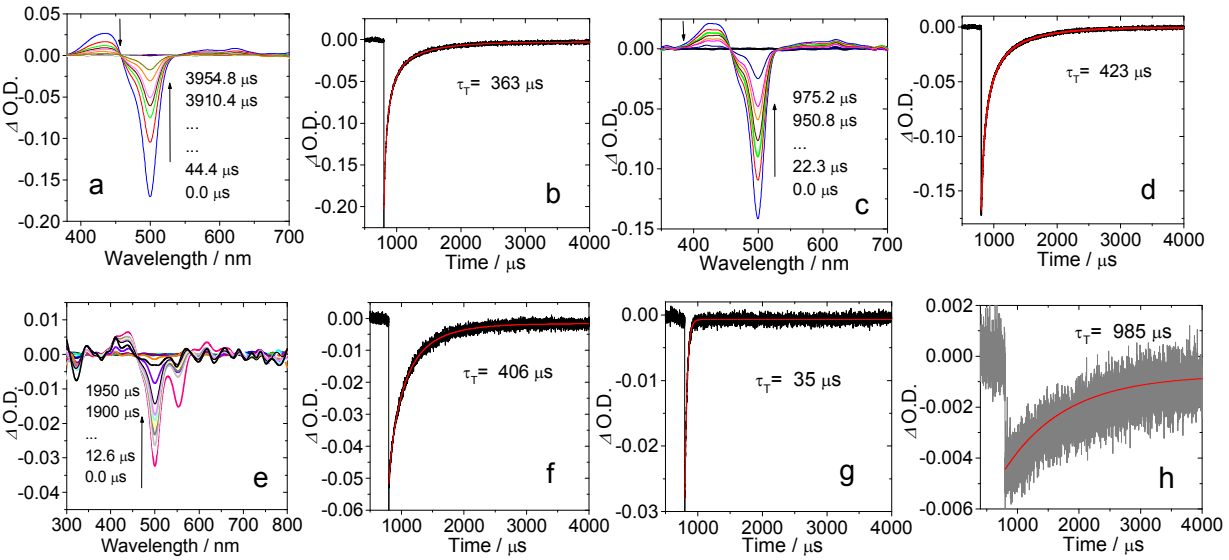

Fig. 9 Nanosecond transient absorption spectra and the decay curves of complexes. (a) Transient absorption spectra of **BDPY-Pt-2** and (b) the corresponding decay curve at 504 nm (λ_{ex} = 500 nm). (c) Transient absorption spectra of **RH-BDPY-Pt-2** and (d) the corresponding decay curves at 504 nm (λ_{ex} = 500 nm). (e) Transient absorption spectra of **RH-BDPY-Pt-2**+TFA (333 eqv.) and (f) the corresponding curve at 504 nm (λ_{ex} = 500 nm), (g) decay curve of **RH-BDPY-Pt-2**+TFA (333 eqv.) at 557 nm (λ_{ex} = 532 nm), (h) decay curve of **RH-Pt**+TFA (333 eqv.) at 554 nm (λ_{ex} = 532 nm). c = 1.0 ×10^{-5} M in deaerated dichloromethane, 20 °C.

Electrochemical study: cyclic voltammetry

The redox potentials of the complexes and the references were studied with cyclic voltammetry (Fig. 10). For **RH-Pt,** irreversible oxidation waves at +0.67 V, +0.79 V and +1.00 V were observed (see ESI †, Fig. S24). No reduction waves were observed. For **BDPY-Pt-1,** reversible oxidation wave at +0.62 V was observed. A reversible reduction wave at −1.55 V was observed. For **BDPY-Pt-2,** an irreversible oxidation wave at +0.93 V was observed.

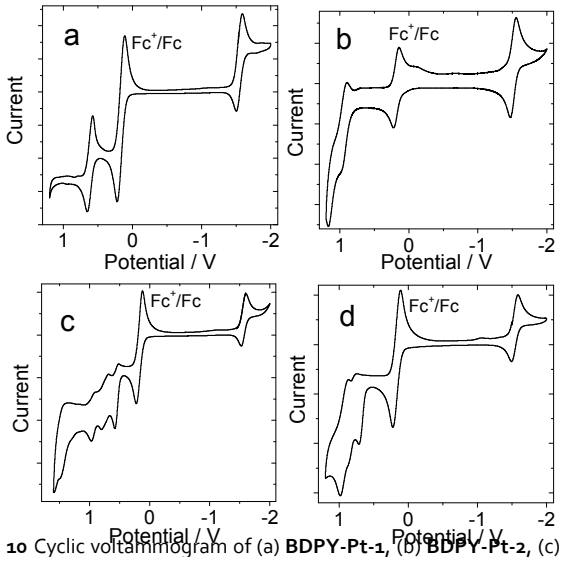

Fig. 10 Cyclic voltammogram of (a) **BDPY-Pt-1,** (b) **BDPY-Pt-2,** (c) **RH-BDPY-Pt-1,** (d) **RH-BDPY-Pt-2**. In deaerated CH_2Cl_2 solutions containing 1.0 mM photosensitizers with the ferrocene (Fc) as internal reference, 0.10 M Bu_4NPF_6 as supporting electrode, $Ag/AgNO_3$ as reference electrode. Scan rates: 0.1 V/s. 20 °C.

The reduction wave at −1.51 V is similar to that of **BDPY-Pt-1**. For **RH-BDPY-Pt-1,** the oxidation waves are basically the sum of the oxidation potential of **BDPY-Pt-1** and **RH-Pt,** thus we propose that there is no significant interaction between the two chromophores at ground state. An reversible reduction wave at −1.55 V was observed, which can be attributed to the coordinated Bodipy ligand. Similar results were observed for **RH-BDPY-Pt-2**. The redox potentials were listed in Table 2.

The free energy changes of the intramolecular electron transfer (ET) process, can be calculated with the Weller equation (Eq. 2 and Eq. 3).[44a]

$$\Delta G^{0}{}_{CS} = e[E_{OX} - E_{RED}] - E_{00} + \Delta G_S \qquad \text{(Eq. 2)}$$

$$\Delta G_S = -\frac{e^2}{4\pi\varepsilon_S\varepsilon_0 R_{CC}} - \frac{e^2}{8\pi\varepsilon_0}\left(\frac{1}{R_D}+\frac{1}{R_A}\right)\left(\frac{1}{\varepsilon_{REF}}-\frac{1}{\varepsilon_S}\right) \qquad \text{(Eq. 3)}$$

Where ΔG_S is the static Coulombic energy, which is described by eq. 3. e is electronic charge, E_{OX} is the half-wave potential for one-electron oxidation of the electron-donor unit, E_{RED} = half-wave potential for one-electron reduction of the electron-acceptor uni; E_{00} = energy level approximated with the fluorescence emission (for the singlet excited state), ε_S = static dielectric constant of the solvent, R_{CC} = center-to-center separation distance between the electron donor (rhodamine unit) and electron acceptor (**BDPY-Pt-1**), determined by DFT optimization of the geometry, R_{CC} (**RH-BDPY-Pt-1**) = 15.1 Å, R_{CC} (**RH-BDPY-Pt-2**) = 16.6 Å, R_D is the radius of the electron donor, R_A is the radius of the electron acceptor, ε_{REF} is the static dielectric constant of the solvent used for the electrochemical studies, ε_0 is permittivity of free space. The solvents used in the calculation of free energy of the ET is dichloromethane (ε_S = 8.93) and toluene (ε_S = 2.4). Charge recombination energy

Table 2. Redox potentials of photosensitizers for study of the potential intramolecular electron transfer by the estimation of free-energy changes for the charge separation ΔG_{CS} (photoinduced electron transfer). Anodic and cathodic peak potential were presented [a]

	$E_{(OX)}$ (V)	$E_{(RED)}$ (V)	ΔG_s(eV)	ΔG_{cs}(eV)[c]	ΔG_{CR}(eV)[c]	ΔG_{cs}(eV)[d]	ΔG_{CR}(eV)[d]
RH-Pt	+0.67/+0.79/+1.00	–[b]	–[b]	–[b]	–[b]	–[b]	–[b]
BDPY-Pt-1	+0.62	−1.55	–[b]	–[b]	–[b]	–[b]	–[b]
BDPY-Pt-2	+0.93	−1.51	–[b]	–[b]	–[b]	–[b]	–[b]
RH-BDPY-Pt-1	+0.94/+0.75/+0.55	−1.55	−0.11[c]/ +0.44[d]	+0.48[e]	−1.99[e]	+1.03[e]	−2.54[e]
				+0.09[f]	−1.99[f]	+0.64[f]	−2.54[f]
RH-BDPY-Pt-2	+0.93/+0.72	−1.54	−0.10[c]/ +0.26[d]	+0.56[e]	−2.16[e]	+0.92[e]	−2.52[e]
				−0.26[f]	−2.16[f]	+0.10[f]	−2.52[f]

[a] Cyclic voltammetry in deaerated CH_2Cl_2 containing 0.10 M Bu_4NPF_6 as supporting electrolyte; Pt electrode as counter electrode; glassy carbon electrode as working electrode; $Ag/AgNO_3$ couple as the reference electrode. *c* [Ag^+] = 0.1 M. 1.0 mM photosensitizers in DCM, 20 °C. Conditions: 1.0 mM dyad photosensitizers and 1.0 mM ferrocene in DCM. [b] No reduction waves was observed, no ΔGcs and no ΔG_{CR} values. [c] In dichloromethane. [d] In toluene. E_{00} of complexes was approximated by the energy levels of the excited states of [e] ^{3}BDPY* and [f] ^{1}BDPY*.

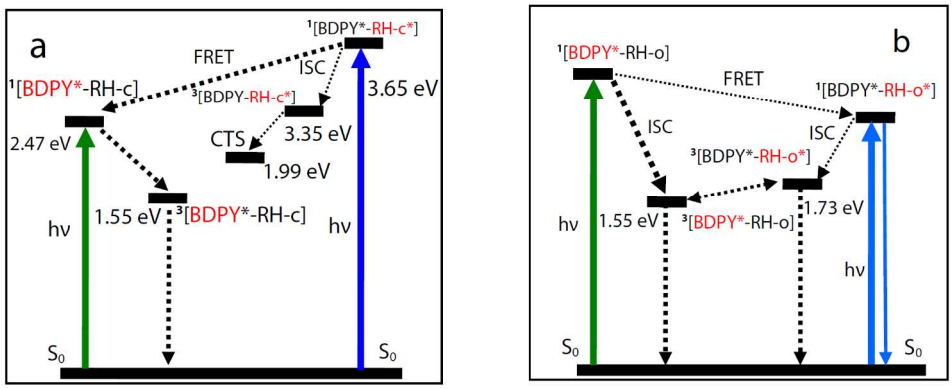

Scheme 2. Simplified Jablonski diagram illustrating the photophysical processes involved in (a) **RH-BDPY-Pt-1** (b) **RH-BDPY-Pt-1** in the presence of TFA in dichloromethane. [BDPY-RH-c] stands for **RH-BDPY-Pt-1** with the rhodamine part in the closed spirolactam structure. [BDPY-RH-c] stands for **RH-BDPY-Pt-1** with the rhodamine part in the opened amide structure. The component at the excited state was selected with red colour. The number of the superscript designates either the singlet or the triplet excited state.

state ($\Delta G_{(CR)}$) can be calculated with the Eq. 4. The data were represented in Table 2.

$$\Delta G_{CR} = -(\Delta G_{CS} + E_{00}) \quad \text{(Eq. 4)}$$

Based on the free energy changes (Table 2), ET is unlikely to occur due to the large positive ΔG_{CR} values. This conclusion is in agreement with the experimental results of the photoluminescence study which show no quenching effect in toluene as compared with that in other polar solvents. In DCM, however, either negative free energy changes or a small positive value were obtained, indicating that ET is possible for both **RH-BDPY-Pt-1** and **RH-BDPY-Pt-2**. Accordingly, luminescence quenching was observed for **RH-BDPY-Pt-1** and **RH-BDPY-Pt-2** in DCM as compared with that in toluene. Moreover, in DCM both **RH-BDPY-Pt-1** and **RH-BDPY-Pt-2** show shorter triplet state lifetimes (Fig. 8 and Fig. 9) as compared with that in nonpolar solvents such as toluene (Fig. 7).

The photophysics of **RH-BDPY-Pt-1** and **RH-BDPY-Pt-2** are presented in Scheme 2. Based on the UV–Vis absorption/fluorescence spectroscopy and the DFT/TDDFT calculated data, both the singlet and the triplet excited states of the closed lactam form of rhodamine part is with higher energy levels than that of the BDPY part. In the presence of TFA, the energy level of the S_1 state of Bodipy part is with higher energy than that of S_1 state of opened rhodamine part.

DFT calculations: assignment of the excited states

The electronic state of the complexes were studied with DFT calculations.[19,46] The results of **RH-BDPY-Pt-2** were presented in Fig. 11 and Table 3. The frontier molecular orbitals were presented in Fig. 11. The S_1 state of the complex (in DCM) was identified as a charge transfer state. The main components of the transition is HOMO→LUMO, which is ET from the rhodamine moiety to the Bodipy moiety, as well as HOMO−2→LUMO, which is charge transfer from the phenylacetylide moiety to the Bodipy moiety. This ET feature supports the experimental results that the fluorescence of **RH-BDPY-Pt-2** was quenched as compared with that in toluene (Fig. 4d).

The triplet state of **RH-BDPY-Pt-2** was also studied with TDDFT calculations (Table 3). T_1 state is a Bodipy-localized ^{3}IL state (Fig. 11). The rhodamine unit and the Pt(II) coordination centre do not contribute to the T_1 state. This conclusion is in agreement with the nanosecond transient absorption spectroscopy which shows that the T_1 state of **RH-BDPY-Pt-2** is exclusively localized on the Bodipy moiety (Fig. 9c).

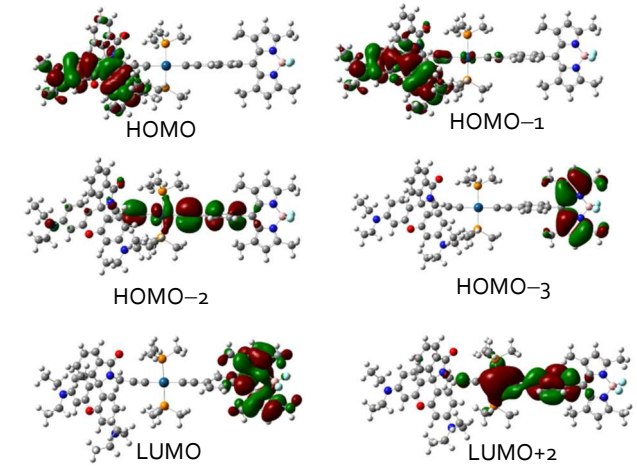

Fig. 11 Electron density maps of the frontier molecular orbital of the complex **RH-BDPY-Pt-2** in dichloromethane. Based on the optimized ground state geometry by the DFT calculations at the B3LYP/GENECP level with Gaussian 09W.

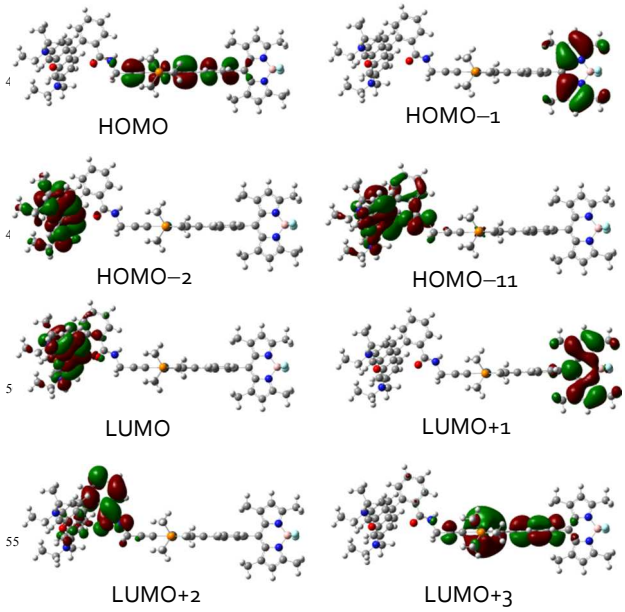

Fig. 12 Electron density maps of the frontier molecular orbital of the complex **RHO-BDPY-Pt-2 (open amide form)** in dichloromethane Based on ground state optimized geometry by the DFT calculations at the B3LYP/GENECP level with Gaussian 09W.

The excited states of **RH-BDPY-Pt-2** with the rhodamine moiety in the opened amide structure were also studied (Fig. 12 and Table 4). Two low-lying singlet states were recognized for **RH-BDPY-Pt-2,** which are localized on rhodamine moiety (S_4 state) and the Bodipy moiety (S_6 state), respectively. We noted the discrepancy between the calculated excitation energy and the experimental UV-Vis absorption of the complex in the presence of TFA (Fig. 2b), however, the trend is correct.[46,47]

The triplet states of **RH-BDPY-Pt-2** with the rhodamine moiety in the opened amide structure were studied with the TDDFT calculations. We found that T_1 state is localized on the Bodipy moiety (1.54 eV), with HOMO−1→LUMO+1 as the component of the transition (Fig. 12). T_2 state is localized on the Rhodamine moiety with opened amide structure, HOMO−2→LUMO is involved in the transition (Fig. 12). Notably the energy level of T_2 (1.74 eV) is only slightly higher than that of T_1 (1.54 eV), thus population of both T_1 and T_2 states is possible. This postulation was confirmed by the nanosecond transient absorption spectra of **RH-BDPY-Pt-2** (Fig. 9e), in which both the bleaching bands of the Bodipy and the rhodamine moiety were observed. Thus the photophysical properties of **RH-BDPY-Pt-2** were fully rationalized by the DFT and the TDDFT calculations. Similar studies were carried out for **RH-BDPY-Pt-1** (please refer to ESI†).

Table 3. Electronic excitation energies (eV) and corresponding oscillator strengths (*f*), main configurations and CI coefficients of the low-lying electronic excited states of the complex **RH-BDPY-Pt-2** in dichloromethane calculated by TDDFT//B3LYP/GENECP based on the DFT//B3LYP/ GENECP optimized ground state geometries.

	TDDFT//B3LYP/ GENECP					
	Electronic transition	Energy [eV/nm] [a]	*f* [b]	Composition [c]	CI [d]	Character
Singlet	$S_0 \rightarrow S_1$	2.48/499	0.002	H−2→L	0.535	MLCT
				H→L	0.419	LLCT
	$S_0 \rightarrow S_5$	2.89/429	0.589	H−3→L	0.700	ILCT
	$S_0 \rightarrow S_8$	3.42/363	0.064	H−3→L	0.121	ILCT
	$S_0 \rightarrow S_{15}$	3.97/312	0.498	H−2→L+2	0.497	MLCT
				H−1→L+2	0.221	MLCT
Triplet	$S_0 \rightarrow T_1$	1.54/805	0.000	H−3→L	0.710	ILCT
	$S_0 \rightarrow T_2$	2.48/501	0.000	H−2→L	0.575	MLCT
				H→L	0.346	LLCT
	$S_0 \rightarrow T_3$	2.51/494	0.000	H→L	0.601	LLCT
	$S_0 \rightarrow T_4$	2.62/473	0.000	H−2→L	0.651	MLCT

[a] Only the selected low-lying excited states are presented. [b] Oscillator strengths. [c] Only the main configurations are presented. [d] The CI coefficients are in absolute values. [e] No spin-orbital coupling effect was considered, thus the *f* values are zero.

Cite this: DOI: 10.1039/coxx00000x

www.rsc.org/xxxxxx

PAPER

Table 4. Electronic excitation energies (eV) and corresponding oscillator strengths (*f*), main configurations and CI coefficients of the low-lying electronic excited states of the complex **RH(o)-BDPY-Pt-2** (rhodamine part in the open amide form) in dichloromethane calculated by TDDFT//B3LYP/GENECP based on the DFT//B3LYP/ GENECP optimized ground state geometries.

	TDDFT//B3LYP/ GENECP					
	Electronic transition	Energy / eV/nm [a]	*f* [b]	Composition [c]	CI [d]	Character
Singlet	$S_0 \rightarrow S_1$	2.22/558	0.002	H→L	0.705	MLCT
	$S_0 \rightarrow S_4$	2.61/476	0.978	H−2→L	0.702	ILCT
	$S_0 \rightarrow S_6$	2.89/429	0.596	H−1→L+1	0.700	ILCT
	$S_0 \rightarrow S_{15}$	3.54/350	0.114	H−11→L	0.493	ILCT
	$S_0 \rightarrow S_{17}$	3.62/343	0.365	H−11→L	0.382	ILCT
				H→L+2	0.165	MLCT
				H→L+3	0.136	MLCT
	$S_0 \rightarrow S_{22}$	3.76/330	0.489	H→L+3	0.549	MLCT
				H→L+2	0.341	MLCT
Triplet	$S_0 \rightarrow T_1$	1.54/806	0.000	H−1→L+1	0.710	ILCT
	$S_0 \rightarrow T_2$	1.74/713	0.000	H−2→L	0.705	ILCT
	$S_0 \rightarrow T_3$	2.22/559	0.000	H→L	0.705	MLCT
	$S_0 \rightarrow T_4$	2.37/522	0.000	H−1→L	0.707	LLCT

[a] Only the selected low-lying excited states are presented. [b] Oscillator strengths. [c] Only the main configurations are presented. [d] The CI coefficients are in absolute values. [e] No spin-orbital coupling effect was considered, thus the *f* values are zero.

Conclusion

In conclusion, the UV–Vis absorption, photoluminescence and the triplet state lifetimes of trans bis(tributylphosphine) Pt(II) bisacetylide complexes were switched by acid (trifluoroacetic acid, TFA). The aim of this research is to switch the photophysical properties of transition metal complexes with external stimuli. Herein the acid-activatable chromophore rhodamine coordinated with Pt(II) was used for this purpose for the first time. Moreover, Bodipy acetylide ligands were used for achieving strong absorption of visible light. The photophysical properties of the complexes were studied with steady state UV–Vis absorption spectra, luminescence spectra, nanosecond transient absorption spectroscopy, electrochemical characterization and DFT/TDDFT computations. The complexes show the featured absorption bands of the coordinated Bodipy ligands. Upon addition of acid, new absorption bands assigned to the open amide structure of the rhodamine moiety were observed, accordingly colour changes was observed for the solutions. The fluorescence of the complexes were enhanced upon addition of acid. Furthermore, for one of the Pt(II) complex the triplet state lifetime was extended upon addition of acid. For another complex, switching from a Bodipy-confined triplet state to a triplet state delocalized on both the Bodipy and the rhodamine ligands was observed. The photophysical properties were rationalized with DFT/TDDFT calculations. Such tuning of the photophysical properties of Pt(II) complexes with rhodamine moiety was reported for the first time and these results may be useful for future designing of external-activatable triplet photosensitizers.

Acknowledgements

We thank the NSFC (21273028, 51202207, 21473020 and 21421005), the Royal Society (UK) and NSFC (China-UK Cost-Share Science Networks, 21011130154), Program for Changjiang Scholars and Innovative Research Team in University [IRT_13R06], State Key Laboratory of Fine Chemicals (KF1203), the Fundamental Research Funds for the Central

Universities (DUT14ZD226) and Dalian University of Technology (DUT2013TB07) for financial support.

Note and references

State Key Laboratory of Fine Chemical, School of Chemical Engineering, Dalian University of Technology, Dalian, 116024, P.R. China. Fax: (+86) 411-8498-6236; E-mail: zhaojzh@dlut.edu.cn;
Web : http://finechem2.dlut.edu.cn/photochem

† Electronic Supplementary Information (ESI) available: ^{1}H NMR, ^{13}C NMR, and HRMS spectra of the compounds, and photophysical data of the ligabds and complexes and coordinates of the optimized geometries of the complexes. See DOI: 10.1039/boooooox/

1 A. Kamkaew, S. H. Lim, H. B. Lee, L. V. Kiew, L. Y. Chung and K. Burgess, *Chem. Soc. Rev.*, 2013, **42**, 77–88.
2 S. G. Awuah and Y. You , *RSC Adv.*, 2012, **2**, 11169–11183.
3 (*a*) Y. You and W. Nam , *Chem. Soc. Rev.*, 2012, **41**, 7061–7084; (*b*) Y. Feng, J. Cheng, L. Zhou, X. Zhou, H. Xiang, *Analyst*, 2012, **137**, 4885–4901.
4 J. Zhao, W. Wu, J. Sun and S. Guo, *Chem. Soc. Rev.*, 2013, **42**, 5323–5351.
5 D. P. Hari and B. Konig, *Angew. Chem. Int. Ed.*, 2013, **52**, 4734–4743.
6 (*a*) L. Shi and W. Xia, *Chem. Soc. Rev.*, 2012, **41**, 7687–7697; (*b*) G. Zhao, C. Yang, L. Guo, H. Sun, C. Chen, W. Xia, *Chem. Commun.*, 2012, **48**, 2337–2339; (*c*) G. Zhao, C. Yang, L. Guo, H. Sun, R. Lin, W. Xia, *J. Org. Chem.*, 2012, **77**, 6302−6306; (*d*) D. Ravelli, M. Fagnoni and A. Albini, *Chem. Soc. Rev.*, 2013, **42**, 97–113.
7 (*a*) T. Lazarides, T. M. McCormick, K. C. Wilson, S. Lee, D. W. McCamant and R. Eisenberg, *J. Am. Chem. Soc.*, 2011, **133**, 350–364;

(*b*) R. P. Sabatini, B. Zheng, W.-F. Fu, D. J. Mark, M. F. Mark, E. A. Hillenbrand, R. Eisenberg and D. W. McCamant. *J. Phys. Chem. A*, 2014, **118**, 10663–10672.

8 (*a*) S. Erbas-Cakmak and E. U. Akkaya, *Angew. Chem. Int. Ed.*, 2013, **52**, 11364–11368; (*b*) S. Erbas-Cakmak, O. A. Bozdemir, Y. Cakmak and E. U. Akkaya, *Chem. Sci.*, 2013, **4**, 858–862;

9 (*a*) Y. Sun, Z. M. Hudson, Y. Rao, S. Wang. *Inorg. Chem.*, 2011, **50**, 3373–3378; (*b*) S. Silvi, E. C. Constable, C. E. Housecroft, J. E. Beves, E. L. Dunphy, M. Tomasulo, F. M. Raymo, A. Credi. *Chem. Commun.*, 2009, 1484–1486; (*c*) P. Wu, E. L.-M. Wong, D.-L. Ma, G. S.-M. Tong, K.-M. Ng, C.-M. Che. *Chem. Eur. J.* 2009, **15**, 3652–3656; (*d*) S. K. Brayshaw, S. Schiffers, A. J. Stevenson, S. J. Teat, M. R. Warren, R. D. Bennett, I. V. Sazanovich, A. R. Buckley, J. A. Weinstein, and P. R. Raithby. *Chem. Eur. J.,* 2011, **17**, 4385–4395; (*e*) B.-B. Cui, C.-J. Yao, J. Yao, Y.-W. Zhong. *Chem. Sci.*, 2014, **5**, 932–941; (*f*) Y.-M. Zhang, S.-H. Wu, C.-J. Yao, H.-J. Nie, Y.-W. Zhong. *Inorg. Chem.*, 2012, **51**, 11387–11395; (*g*) C.-J. Yao, Y.-W. Zhong, J. Yao, *J. Am. Chem. Soc.*, 2011, **133**, 15697–15706.

10 T. Yogo, Y. Urano, Y. Ishitsuka, F. Maniwa and T. Nagano, *J. Am. Chem. Soc.*, 2005, **127**, 12162–12163.

11 S. O. McDonnell, M. J. Hall, L. T. Allen, A. Byrne, W. M. Gallagher and D. F. O'Shea, *J. Am. Chem. Soc.*, 2005, **127**, 16360–16361.

12 J. Tian, L. Ding, H.-J. Xu, Z. Shen, H. Ju, L. Jia, L. Bao and J.-S. Yu, *J. Am. Chem. Soc.*, 2013, **135**, 18850–18858.

13 (*a*) A. M. Bugaj, *Photochem. Photobiol. Sci.*, 2011, **10**, 1097–1109; (*b*) P. Majumdar, R. Nomula and J. Zhao, *J. Mater. Chem. C*, 2014, **2**, 5982–5997.

14 D. Hablot, A. Harriman and R. Ziessel, *Angew. Chem. Int. Ed.*, 2011, **50**, 7833–7836.

15 W. Tan, Q. Zhang, J. Zhang and H. Tian, *Org. Lett.*, 2009, **11**, 161–164.

16 M. N. Roberts, C.-J. Carling, J. K. Nagle, N. R. Branda and M. O. Wolf, *J. Am. Chem. Soc.*, 2009, **131**, 16644–16645.

17 Y. Wu, Y. Xie, Q. Zhang, H. Tian, W. Zhu and A. D. Q. Li, *Angew. Chem. Int. Ed.*, 2014, **53**, 2090–2094.

18 L. Hou, X. Zhang, T. C. Pijper, W. R. Browne and B. L. Feringa**,** *J. Am. Chem. Soc.,* 2014, **136**, 910–913.

19 J. Boixel, V. Guerchais, H. L. Bozec, D. Jacquemin, A. Amar, A. Boucekkine, A. Colombo, C. Dragonetti, D. Marinotto, D. Roberto, S. Righetto and R. D. Angelis, *J. Am. Chem. Soc.,* 2014, **136**, 5367–5375.

20 M. Irie, *Chem. Rev.,* 2000, **100**, 1685–1716.

21 M. H. Lee, J. H. Han, J. H. Lee, N. Park, R. Kumar, C. Kang and J. S. Kim, *Angew. Chem. Int. Ed.*, 2013, **52**, 6206–6209.

22 J. Fan, M. Hu, P. Zhan and X. Peng, *Chem. Soc. Rev.*, 2013, **42**, 29–43.

23 X. Chen, Y. Zhou, X. Peng and J. Yoon, *Chem. Soc. Rev.*, 2010, **39**, 2120–2135.

24 X. Zhang, Y. Xiao and X. Qian, *Angew. Chem. Int. Ed.*, 2008, **47**, 8025–8029.

25 L. Huang, L. Zeng, H. Guo, W. Wu, W. Wu, S. Ji and J. Zhao, *Eur. J. Inorg. Chem.,* 2011, **2011**, 4527–4533.

26 W. Wu, J. Zhao, J. Sun, L. Huang and X. Yi, *J. Mater. Chem. C.*, 2013, **1**, 705–716.

27 G. Ulrich, R. Ziessel and A. Harriman, *Angew. Chem. Int. Ed.*, 2008, **47**, 1184–1201.

28 R. Ziessel and A. Harriman, *Chem. Commun.*, 2011, **47**, 611–631.

29 M. J. Frisch, et al., *Gaussian 09*, Revision 01, Gaussian Inc., Wallingford, CT, 2009.

30 A. P. de Silva, H. Q. N. Gunaratne, T. Gunnlaugsson, A. J. M. Huxley, C. P. McCoy, J. T. Rademacher, and T. E. Rice, *Chem. Rev.*, 1997, **97**, 1515–1566.

31 A. M. Soliman, M. Abdelhameed, E. Zysman-Colman and P. D. Harvey, *Chem. Commun.*, 2013, **49**, 5544–5546.

32 C. K. M. Chan, C.-H. Tao, K.-F. Li, K. M.-C. Wong, N. Zhu, K.-W. Cheah and V. W.-W. Yam, *Dalton Trans.*, 2011, **40**, 10670–10685.

33 C. K. M. Chan, C.-H. Tao, H.-L. Tam, N. Zhu, V. W.-W. Yam and K.-W. Cheah, *Inorg. Chem.*, 2009, **48**, 2855–2864.

34 J. E. Rogers, J. E. Slagle, D. M. Krein, A. R. Burke, B. C. Hall, A. Fratini, D. G. McLean, P. A. Fleitz, T. M. Cooper, M. Drobizhev, N. S. Makarov, A. Rebane, K.-Y. Kim, R. Farley and K. S. Schanze, *Inorg. Chem.*, 2007, **46**, 6483–6494.

35 W.-Y. Wong and C.-L. Ho, *Coord. Chem. Rev.*, 2006, **250**, 2627–2690.

36 L. Yuan, W. Lin, Y. Yang and H. Chen, *J. Am. Chem. Soc.,* 2012, **134**, 1200−1211.

37 (*a*) K. Feng, M.-L. Yu, S.-M. Wang, G.-X. Wang, C.-H Tung and L.-Z. Wu, *ChemPhysChem*, 2013, **14**, 198–203; (*b*) J. Chen, S. Li, L. Zhang, B. Liu, Y. Han, G. Yang and Y. Li, *J. Am. Chem. Soc.*, 2005, **127**, 2165–2171; (*c*) A. A. Rachford, R. Ziessel, T. Bura, P. Retailleau and F. N. Castellano, *Inorg. Chem.*, 2010, **49**, 3730–3736.

38 (*a*) M. T. Whited, P. I. Djurovich, S. T. Roberts, A. C. Durrell, C. W. Schlenker, S. E. Bradforth and M. E. Thompson, *J. Am. Chem. Soc.*, 2011, **133**, 88–96; (*b*) J. A. G. Williams, *Top. Curr. Chem.*, 2007, **281**, 205–268.

39 W. Wu, H. Guo, W. Wu, S. Ji and J. Zhao, *J. Org. Chem.*, 2011, **76**, 7056–7064.

40 W. Wu, J. Zhao, J. Sun and S. Guo, *J. Org. Chem.*, 2012, **77**, 5305–5312.

41 (*a*) R. Ziessel, B. D. Allen, D. B. Rewinska and A. Harriman, *Chem. Eur. J.*, 2009, **15**, 7382–7393. (*b*) J.-Y. Liu, M. E. El-Khouly, S. Fukuzumi and D. K. P. Ng, *Chem. Asian J.*, 2011, **6**, 174–179.

42 (*a*) S. Ji, W. Wu, W. Wu, P. Song, K. Han, Z. Wang, S. Liu, H. Guo and J. Zhao, *J. Mater. Chem.*, 2010, **20**, 1953–1963; (*b*) N. D. McClenaghan, Y. Leydet, B. Maubert, M. T. Indelli and S. Campagna, *Coord. Chem. Rev.*, 2005, **249**, 1336–1350; (*c*) J. E. Yarnell, J. C. Deaton, C. E. McCusker and F. N. Castellano*, Inorg. Chem.*, 2011, **50**, 7820–7830.

43 C. Adamo and D. Jacquemin, *Chem. Soc. Rev.*, 2013, **42**, 845–856.

44 A. Vlcek Jr. and S. Zalis, *Coord. Chem. Rev.*, 2007, **251**, 258–287.

45 D. T. Chase, B. S. Young and M. M. Haley*, J. Org. Chem.*, 2011, **76**, 4043–4051.

46 W. Wu, L. Liu, X. Cui, C. Zhang and J. Zhao, *Dalton Trans.*, 2013, **42**, 14374–14379.

Graphical Abstract

Switching of the photophysical properties of Bodipy-derived trans bis(tributylphosphine) Pt(II) bisacetylide complexes with rhodamine as the acid-activatable unit

Poulomi Majumdar, Xiaoneng Cui, Kejing Xu and Jianzhang Zhao*

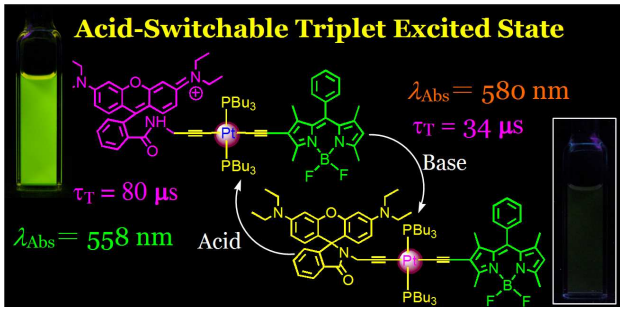

Rhodamine moiety was used in two Bodipy-derived trans bis(tributylphosphine) Pt(II) bisacetylide complexes for switching the photophysical properties of the complexes.